RSC Advances




ROYAL SOCIETY OF CHEMISTRY

www.rsc.org/advances

# The Microscopic mechanism in the realization of the ultra-wide temperature stability in $Bi^{3+}$,$Na^{+}$,$Zn^{2+}$,$Nb^{5+}$ doped $BaTiO_3$ dielectric system

Bowen Zhang, Lingxia Li†,

*School of Electronic and Information Engineering, Tianjin University, Tianjin 300072, China*

**Abstract**

A novel lead-free, high dielectric constant, ultra-wide temperature stable dielectric ceramic was prepared by traditional solid-state reaction method. The microscopic mechanism, electric and dielectric properties of the $Bi^{3+}$,$Na^{+}$,$Zn^{2+}$,$Nb^{5+}$ doped $BaTiO_3$ dielectric system were investigated for the first time. X-ray diffraction revealed that $Bi^{3+}$,$Na^{+}$,$Zn^{2+}$,$Nb^{5+}$ and $BaTiO_3$ form a solid-solution with the pseudo-cubic structure. The thermal vibration and the interaction between the dipoles contributing to the realization of the ultra-wide temperature stability, was discussed. The microscopic model based on the bond energy and coordination number, was used to research on changes of the dielectric stability. In this paper, the contacts between microscopic mechanism and the macroscopic dielectric properties in the ultra-wide temperature stable dielectric ceramics was established, thereby paving the way for achieving ultra-wide temperature capacitors. In addition, fine dielectric properties of $(Na_{0.015}Bi_{0.3}Ba_{0.685})(Zn_{0.2}Nb_{0.115}Ti_{0.685})O_3$ with ε r of 700, tan δ of 0.00535 can be obtained over a ultra-wide temperature range (-53~350$^{o}$C).These features made the ceramics system have high practical values in the miniaturization and increasing applications in harsh environments.

**Key words:** Microstructure; Microscopic model; Microscopic mechanism; Ceramics; Ultra-wide temperature stability.

†Corresponding author. Tel./fax:+86 22 27402838
Email address: llxtju@126.com (L. Li)

## 1.Introduction

The rapid development of the electronics industry puts forward higher requirements for the next generation of dielectric ceramic materials[1-4]. With the increasing integration of components, more circuits and devices are integrated in a limited space. A high dielectric constant are required for the capacitor, so that it can meet the requirements of miniaturization. What's more, the needs for short circuit length force us to make the circuit module near or directly in the work environment. Harsh working conditions, such as automobile engines, rocket , as well as outer space, require the components can be stable in the ultra-broad temperature scope[1-4].The ceiling working temperature of the dielectric materials is raised from 125$^{o}$C (Electronic Industries Alliance X7R) to 150$^{o}$C (EIA-X8R) and then reaches to 200$^{o}$C (EIA-X9R)[5-9].

With its high dielectric constant, excellent insulation properties, non-toxicity and low cost, $BaTiO_3$ based ceramics have became one of the major dielectric ceramic materials[10]. The ceiling temperature of present $BaTiO_3$ based dielectric materials only reaches 125-200$^{o}$C. When the temperature increase over 200$^{o}$C, a sharp decline occur. However, even X9R materials would not fulfill the requirements in some harsh conditions, such as oil drilling, aerospace and automotive environment. For example, the anti-lock brake system sensors on wheels are required to work at a temperature range of 150-250$^{o}$C and in the cylinder the ambient temperature is 200-300$^{o}$C. The mismatch between the narrow effective temperature range (125-200$^{o}$C) and the high operating temperature requirements (over 200$^{o}$C) severely limits the use of dielectric components (e.g MLCC). Thus, it is of great significance to develop temperature stable dielectric materials with a high dielectric constant,and low dielectric loss over a wide temperature range (-55~350$^{o}$C)[14-17].

Currently, there are many researches on the development of wide temperature stable dielectric

materials. However, rare studies have been done on microscopic mechanisms in the materials, which benefits the realization of ultra-wide temperature stability. In this paper, we reported $Bi^{3+}$,$Zn^{2+}$,$Nb^{5+}$ doped $BaTiO_3$ dielectric system, which had a high dielectric constant, low dielectric loss over a wide temperature range (-53~350$^{o}$C). The thermal vibration and the interaction between the dipoles contributing to the realization of the ultra-wide temperature stability, was discussed. What's more, the bond energy and coordination number model was used to research on the movements of the temperature stable range. This work have high practical values in the development of ultra-wide temperature stable dielectric ceramics.

**2. Experimental procedures**

Reagent-grade $BaTiO_3$, $Na_2CO_3$, $Bi_2O_3$, ZnO, $Nb_2O_5$ were used as raw materials. Firstly, reagent-grade oxides and carbonate of $Bi_2O_3$, ZnO and $Nb_2O_5$ were weighed with a mole ratio of 3:4:1and mixed using ball-milling in deionized water for 4h. Then the mixture was calcined in air at 800$^{o}$C to synthesize $Bi(Zn_{2/3}Nb_{1/3})O_3$ phase. Secondly, stoichiometric proportions of $Na_2CO_3$ and $Nb_2O_5$ were mixed by ball milling in deionized water for 4 h. The mixture were dried and calcined at 900$^{o}$C in covered alumina crucible for 4h to synthesize $NaNbO_3$ phase. $Bi(Zn_{2/3}Nb_{1/3})O_3$ and $NaNbO_3$ have a similar structure with the $BaTiO_3$[36,38-47]. In the sintering process, it is more convenient for $Bi^{3+}$,$Na^{+}$, $Zn^{2+}$, $Nb^{5+}$ to diffuse into the crystal lattice, rather than the forms of oxide, such as $Bi_2O_3$, ZnO and $Nb_2O_5$. Subsequently, $(1-x)BaTiO_3$-$xBi(Zn_{2/3}Nb_{1/3})O_3$-$0.015NaNbO_3$ ($0.22\leq x\leq 0.30$) powders were weighed and milled in deionized water using zirconia balls for 4 h. The locations of the compositions in the $(1-x)BaTiO_3$-$xBi(Zn_{2/3}Nb_{1/3})O_3$-$0.015NaNbO_3$ system are shown in Figure 1. After drying, the mixed powders were added in 7wt% binder wax, and then cold isostatically pressed into discs under a pressure of 200MPa with 20mm in diameter and 1mm in thickness. Samples were

sintered at 1200°C for 2h. The samples with x=0.22, 0.24, 0.0.27, 0.30 were named Sample 1, Sample 2, Sample 3, Sample 4, respectively.

Crystal structure of the samples was identified at room temperature using an X-ray diffractometer (D8-Focus, Bruker AXS GmbH, German). To reduce noise, all data have been smoothed by Adaptive smoothing method and had deducted background. All parameters including background, zero-point, scale factors for all phases, half-width, asymmetry parameters, unit-cell parameters, atomic positional coordinates, temperature factors are refined step-by-step for avoiding correlations by the soft-ware of Fullprof-suite. Microstructure of the ceramic samples was observed by field emission scanning electron microscopy (FE-SEM, S-4800, Hitachi, Ltd. Japan). Dielectric loss and capacitance were measured by the use of capacitance meter (HP4278A) at 1KHz~1MHz, with temperature range of -55°C to 350°C. Insulation resistance was measured using a high resistance meter (Agilent 4339B) at room temperature.

**3. Results and Discussion**

**3.1 The micro-mechanism and the dielectric properties**

Figure 2(a)-(c) shows the temperature dependence of dielectric constant and capacitance variation rate based on $C_{25^oC}$ with various amounts of $Bi^{3+}$,$Na^{+}$,$Zn^{2+}$,$Nb^{5+}$, sintered at 1200°C, measured at 1kHz~1MHz. As Figure 2 shows that only one dielectric dispersion peak at the low temperature (~25°C) and the dielectric constant varies with frequency, which is consistent with the relaxation ferroelectrics. The"modified Curie-Weiss law"[34] is a method commonly used in the study of ferroelectric materials, which is expressed by the following equation:

$$\frac{1}{\varepsilon}-\frac{1}{\varepsilon_m}=\frac{(T-T_m)^{\gamma}}{C}$$

Where ε is the relative permittivity, Tm is the temperature,$\varepsilon_m$ is the maximumε value at T=Tm, C is the modified Curie-Weiss constant, and r is a measurement of diffusivity. The material with r=1 fits normal

ferroelectric behavior, with r=2 fits ideal relaxation ferroelectric system[35], and between 1 and 2 indicates a diffuse ferroelectric characteristic, which has the characteristics of "relaxorlike" bahavior. Figure 2(d) shows that the diffuse exponent r is about 1.4~1.5 for the (1-x)$BaTiO_3$-x$Bi(Zn_{2/3}Nb_{1/3})O_3$-0.015$NaNbO_3$ ($0.22\leq x\leq 0.30$) ceramics, which confirmed that the (1-x)$BaTiO_3$-x$Bi(Zn_{2/3}Nb_{1/3})O_3$-0.015$NaNbO_3$ exhibit the "relaxorlike" behavior. It was the special structure—"relaxorlike" that makes $Bi^{3+}$,$Na^{+}$,$Zn^{2+}$,$Nb^{5+}$ doped $BaTiO_3$ dielectric system with special dielectric properties. The details are shown as below[35].

The spontaneous polarization existed in the ferroelectric $BaTiO_3$ and the long-range interactions between the dipoles promoted the dipoles to form ferroelectric domain. When an external electric field was applied, the ferroelectric domains would be extended along the external electric field, which is the reason for a high dielectric constant in $BaTiO_3$. While, the long-range interactions between dipoles were destroyed by doping of external additives. The macroscopic ferroelectric domains gradually decreased and the randomly distributed micro-domains formed[18-20]. Figure 3 shows the micro-mechanism in the $Bi^{3+}$,$Na^{+}$,$Zn^{2+}$,$Nb^{5+}$ doped $BaTiO_3$ dielectric system, benefiting to the realization of ultra-wide temperature stability.

When an external electric field was applied, there would three forces in the phase change process—external electric field force( $F_e$ ), the interaction between the polarization micro-domains ( $F_i$ ) and the thermal vibration force( $F_v$ ) throughout the whole temperature range. The interaction between the polarization micro-domains and the thermal vibration make the polarization micro-domains distribute randomly and the macroscopic polarization is reduced. While, the external electric field force( $F_e$ ) make the polarization micro-domains distribute along the external electric field and the macroscopic polarization is increased. Local polarization region came in to being at Burns temperature (Td). When

the ambient temperature T >>Td, no polarization existed and dielectric system is paraelectric phase. Burns temperature is generally higher than the temperature Tc where the maximum dielectric constant exist.

In the high temperature range(T≤Td), thermal vibration is very strong. The interactions of different polarization regions($F_i$) is so weak that it can be ignored. Thermal vibration force ($F_v$) is greater than the of the external electric field force(Fe). The polarization micro-domains can vibrate in several equivalent direction. And, the orientation of each polarization micro-domains is insulated from the others. The macroscopic polarization was close to zero.

In the temperature region of Tc <T <<Td, the polarization micro-domains gradually grew up. The thermal vibration($F_v$) is reduced and gradually less than the external electric field force( $F_e$ ). The interactions of different polarization regions(Fi) remain so weak that it can be ignored. Since the temperature is still relative high, the degree of freedom of the polarization micro-domains is high and the external electric field force( $F_e$ ) make the polarization micro-domains distribute along the external electric field quickly. As a result, the dielectric constant increased and the relaxivity is low.

In the temperature region of Tf<<T <Tc, the polarization micro-domains is large, the interaction between the polarization micro-domains is strong. Because the temperature is relative low, the thermal vibration energy is small and it can be ignored. The polarization micro-domains gradually grew up and the interactions of micro-domains became strong when the temperature continues to decline. The electric field directional force(Fe) is gradually less than the the interaction between the polarization micro-domains ($F_i$). As a result, the dielectric constant was decreased ,dielectric loss and relaxivity was enhanced.

In the temperature region of T≥Tf, the polarization micro-domains becomes larger and the

interaction between the dipole (polarization micro-domains)($F_i$) is larger than the electric field directional force($F_e$) which lead dipole distribute randomly. The ambient temperature is so law that thermal vibration can be ignored. As a result, the macroscopic polarization was close to zero.

Accordingly，the dielectric constant increased firstly and then decreased, and significant dielectric relaxation appeared in the low temperature.

**3.2 Bond energy and coordination number relaxor model and the dielectric stability**

In the $Bi^{3+}$,$Na^{+}$,$Zn^{2+}$,$Nb^{5+}$ doped $BaTiO_3$ dielectric system, the relaxation reason from the inert substitution of A, B site ions. $Bi^{3+}$,$Na^{+}$,$Zn^{2+}$,$Nb^{5+}$ diffuses into the cell and the dielectric system changes from the normal ferroelectrics to diffuse ferroelectrics. The relaxation behavior can be described as the relationship of Vogel-Fulcher:

$$f = f_0 \exp[-\frac{E_a}{k(Tc - Tf)}] \qquad (1)$$

f: the measurement frequency; $f_0$: Debye frequency; k: Boltzmann's constant; Tc: the temperature corresponding to the maximum dielectric; Ea: activation energy of the transition in micro-domains; Tf: Freezing temperature of the transition

According to bond energy and coordination number model, the Vogel-Fulcher formula can be expressed as follows[23-24]:

$$\tau = \tau_0 \left\langle \exp(\frac{EZ}{kT}) \right\rangle \qquad (2)$$

$$f = \frac{1}{\tau} = f_0 \left\langle \exp(-\frac{EZ}{kT}) \right\rangle \qquad (3)$$

$\langle\ \rangle$: Statistics average; $\tau$ :Relaxation time; E:The interaction between the neighbors dipoles; Z: The number of neighbors dipole.

In the crystal of BaTiO3, one $Ti^{4+}$ ion and six $O^{2-}$ ions form the special structure of [$TiO_6$]

octahedral, which can be seen in the Figure 1. In the octahedral, $Ti^{4+}$ deviates from the center position of the octahedron and the dipole forms. So, each [$TiO_6$] octahedral can be seen as one dipole.

In the $Bi^{3+}$,$Na^{+}$,$Zn^{2+}$,$Nb^{5+}$ doped $BaTiO_3$ dielectric system, $Bi^{3+}$,$Na^{+}$,$Zn^{2+}$,$Nb^{5+}$ diffuses into the cell. Because of the different radii and valence with $Ba^{2+}$ and $Ti^{4+}$, the doping ions($Zn^{2+}$,$Nb^{5+}$) locate at the center of the oxygen octahedra . As a result, dipole can not forms.

What's more, the original polarized [$TiO_6$] octahedral in BaTiO3 are separated by the non-polarized area (the doping area). As a result, the interactions between the dipoles weakened.

In summary, the inert substitution of A, B site ions makes the number of neighbors dipole decreased and the interactions(which we call them Bond energy in this paper) between the dipoles weakened. Due to the non-uniform distribution of dopant ions[37], different dipole has its own surroundings. Thus, the coordination number and bond energy of each dipole can be described as follows:

$$Z = Z_0 + \Delta Z \qquad (4)$$

$$E = E_0 + \Delta E \qquad (5)$$

$Z_0$: The average coordination number of each dipole in the whole system; $\Delta Z$: Fluctuations in the coordination number of local areas due to the non-uniform distribution of dopant ions; $E_0$: The average bond energy of each dipole in the whole system; $\Delta E$: Fluctuations in bond energy of local areas due to the non-uniform distribution of dopant ions.

When the bond energy and coordination number follows Gaussian distribution [25]

$$\tau = \tau_0 \frac{1}{\sqrt{4\pi^2 \Delta E^2 \Delta Z^2}} \int_{-\infty}^{\infty}\int_{-\infty}^{\infty} \exp\left(\frac{EZ}{kT} - \frac{(E-E_0)^2}{2\Delta E^2} - \frac{(Z-Z_0)^2}{2\Delta Z^2}\right) dEdZ \qquad (6)$$

$$\Delta E / E_0 = \gamma \cdot \Delta Z / Z_0 \qquad (7)$$

When $\gamma$ =1 the formula (7) can be expressed as[26]

$$\ln(f / f_0) = -\frac{E_0 Z_0}{kT_m - (E_0 Z_0)(\Delta E / E_0)^2} \qquad (8)$$

In the $Bi^{3+}$,$Na^{+}$,$Zn^{2+}$,$Nb^{5+}$ doped $BaTiO_3$ dielectric system, the substitution of doping ions within the crystal is non-uniform[37].The non-uniform distribution of the crystal inside lead large fluctuations in bond energy (ΔE). From the Equation(8), we can conclude that the relaxation behavior will be enhanced with the increase of doping content.

What's more, due to the non-uniform distribution of the substitutional ions, the surroundings of each dipoles are different. Different areas have their own activation energy. So, different areas have different responses to temperature. As a result, the dielectric peak was broadened and dielectric stability was enhanced. The mechanism was shown in the Figure 2.

The results of Figure 2-3 and Table1 consist with the discussion above. Figure2 and Table 1 show that from the sample 1 to sample 4，the dielectric stability gradually increased from the range of -55~245$^{o}$C to -53~350$^{o}$C. What's more, according to the Equation (8), if the measuring frequency (f) remains constant, Tc will move to higher temperature with the increasing of the doping content (ΔE is increased). Table 1 shows the dielectric properties of the samples1-4, when the doping content increased from x = 0.24 to x = 0.30 , Tc increased from ~25$^{o}$C increased to ~50$^{o}$C. The movement of Tc make the temperature stable range moving to higher temperature which we can see from the Figure2 and Table 1.

**3.3 Structure of $Bi^{3+}$, $Zn^{2+}$, $Nb^{5+}$ doped $BaTiO_3$ solid solution**

Figure 4(a) shows the X-ray diffraction patterns of (1-x)$BaTiO_3$-x$Bi(Zn_{2/3}Nb_{1/3})O_3$-0.015$NaNbO_3$ doped with different content of $Bi(Zn_{2/3}Nb_{1/3})O_3$ sintered at 1200$^{o}$C. All samples show a perovskite phase, which means that the formation of solid solution between $Bi^{3+}$,$Na^{+}$,$Zn^{2+}$,$Nb^{5+}$ and $BaTiO_3$. No second phase exist. The enlarged XRD patterns in the range of 2θ from 44$^{o}$ to 46$^{o}$ are illustrated in

Figure 4(b). It is clearly visible that the merging of (002)/(200) ($2\theta=45^{o}$) diffraction peaks of the pure barium titanate into a single (200) peak, indicating a transforming from tetragonal phase (P4mm) to Pseudocubic symmetry. Just as what we can see from the dielectric constant-temperature curve mentioned above, the Curie peak at ~120°C(pure $BaTiO_3$) disappeared. In addition, the dielectric anomaly peak occurs at the low temperature ~25°C . Besides, with the increase of the doping concentration of $Bi(Zn_{2/3}Nb_{1/3})O_3$, (200) diffraction peak shifted toward lower angles firstly (from x=0.22 to x=0.24) and then (200) diffraction peak shifted toward higher accompanying by the gradual enhancing $Bi(Zn_{2/3}Nb_{1/3})O_3$ concentration (from x=0.24 to x=0.27, x=0.30). This behavior demonstrates that the lattice parameters of solid solutions increased firstly and then decreased slightly. According to the principles of crystal chemistry and radius-matching rule[30], the incorporation of the radius of $Na^{+}$(1.39Å) and $Bi^{3+}$(1.30Å) are nearly comparable to the value of $Ba^{2+}$ (1.61Å) owing to 12-fold coordination in A-site[27]. While, the B-site ions $Zn^{2+}$ (0.74Å) and $Nb^{5+}$ (0.64Å) are considerably larger radius than that of $Ti^{4+}$ (0.605Å) in six-fold coordination)[28,32]. The substitution of B-site is the main influence factor on the crystal lattice in this paper. When a further increase in $Bi(Zn_{2/3}Nb_{1/3})O_3$ (e.g. sample 3), the content of $Zn^{2+}$ and $Nb^{5+}$ diffuses into the cell is abnormal reduction. This phenomenon is due to the produce of pinning effect by heavily doped $Bi(Zn_{2/3}Nb_{1/3})O_3$, which inhibits the grains' growth. What's more, excessive increase in the content of $Bi(Zn_{2/3}Nb_{1/3})O_3$ (e.g.sample4) will generate a lot of liquid phase in sintering process, the content of $Zn^{2+}$and $Nb^{5+}$ diffuses into the lattice will increase. The lattice parameters (a and c) of the $Bi^{3+}$,$Na^{+}$,$Zn^{2+}$,$Nb^{5+}$ doped $BaTiO_3$ solid solution are calculated based on XRD results using High-Score plus software. Figure 4(c) illustrated the compositional dependence of the tetragonality factor (c/a). The c/a radio reduced from 1.011 for x =0 to 1.0002 for x =0.27 and 0.9971 for x=0.30, became equal to 1. The decreased c/a is

inherently associated with the lower tolerance factor of $Zn^{2+}$and $Nb^{5+}$, which is significantly lower than $Ti^{4+}$ for the pure $BaTiO_3$.

### 3.4 Microstructure of $BaTiO_3$- $Bi(Zn_{2/3}Nb_{1/3})O_3$-$NaNbO_3$ Ceramics

Figure 5 shows the relationships between sintering temperatures and densities of all studied samples. It can be observed that increasing the $Bi(Zn_{2/3}Nb_{1/3})O_3$ content could increase the density while no significant change occurred in sintering temperature. Figure 6 shows the SEM micrographs for $Bi^{3+}$,$Na^{+}$,$Zn^{2+}$,$Nb^{5+}$ doped $BaTiO_3$ dielectric system. As shown in it, the grains are well developed in all the samples. All of the samples show a uniform grain distribution and the size of grain is about 2~3um. No second phase presents in this report. Figure 7 shows the dictribution of the grain size obtained by the software of Nano measure. Just as what we can see, with the increase of the $Bi(Zn_{2/3}Nb_{1/3})O_3$ content, the densification and the grain size increased firstly, then decreased, and increased at last. As mentioned above, the ions $Zn^{2+}$ will enter into the lattice to substitute for $Ti^{4+}$ ions; the imbalance of ion valence will lead to the creation of oxygen vacancies[32-33], which enhances the transfer of mass and energy between the reactants. This improved the sintering process and inducing an increase in the densification of grain distribution. However, a further increase in $Bi(Zn_{2/3}Nb_{1/3})O_3$ ( x=0.30) has an adverse effect on the densification of the samples, as illustrated in Figures 6(c). This phenomenon is due to the produce of pinning effect. When the doping amount is less, the distribution of $Bi^{3+}$,$Na^{+}$,$Zn^{2+}$,$Nb^{5+}$ is uniform. However, when the doping increases, an increase in the number of substitutional ions and lattice distortion increased which is harmful to the diffusion process. Figure 6(d) shows that the densification and the grain size increased again. This may be due to excess doping，a large amount of liquid phase occurred in the sintering process and accumulated in the grain boundaries. The right amount of liquid benefits the dissolution/precipitation process.[27-29,33]

**4. Conclusion**

The crystal structure and dielectric properties of $Bi^{3+}$,$Na^{+}$,$Zn^{2+}$,$Nb^{5+}$ doped $BaTiO_3$ dielectric systems were investigated. The relationship between the microscopic structure and the dielectric properties was discussed systematically. The microscopic model based bond energy and coordination number, was proposed and used to investigate the changes of the dielectric stability in $Bi^{3+}$,$Na^{+}$,$Zn^{2+}$,$Nb^{5+}$ doped $BaTiO_3$ dielectric systems. The obtained results indicated that the doping of $Bi^{3+}$,$Zn^{2+}$,$Nb^{5+}$ can alter the temperature dependence of dielectric constant markedly both in the high and low temperature range, which played a decisive role in the realize of wide temperature range stability. Dielectric measurements showed that the doping of $Bi^{3+}$,$Na^{+}$,$Zn^{2+}$,$Nb^{5+}$ can make the dielectric system change from a normal ferroelectric to a diffusive ferroelectric($1<r<2$), which has the characteristics of normal ferroelectric and ideal relaxation ferroelectric. The temperature coefficient of capacitance was flat in the temperature range of -53~350$^{o}$C . Moreover, the system had a relative higher dielectric constant and lower dielectric loss ($\varepsilon$ r=~700, tan $\delta$=0.00535) over a ultra-wide temperature. These features suggest that the ceramics system can be considered as a promising candidate material for the next generation of MLCC used in the harsh conditions(over 300$^{o}$C).

**References**

[1]R.W. Johnson, J.L. Evans, P. Jacobsen ,J.R. Thompson, M. Christ opher,The changing automotive environment: high-temperature electronics, IEEE Transactions on Electronics Packaging Manufacturing 27 (2004) 164-176.

[2]M.R. Werner, W.R. Fahrner, Review on materials, microsensors, systems and devices for high-temperature and harsh-environment applications, Industrial Electronics, IEEE Transactions on Industrial Electronics 48 (2001) 249-257.

[3]Y. Yuan, C.J. Zhao, X.H. Zhou, B. Tang, S.R. Zhang, High-temperature stable dielectrics in Mn-modi fied (1-x)$Bi_{0.5}Na_{0.5}TiO_3$-x$CaTiO_3$ ceramics, Journal of Electroceramics 25 (2010) 212-217.

[4] J.B. Lim, S. Zhang, N. Kim, T.R. Shrout, High-temperature dielectrics in the

$BiScO_3$-$BaTiO_3$-$(K_{1/2}Bi_{1/2})TiO_3$ ternary system, Journal of the American Ceramic Society 92 (2009) 679-682.

[5] S. Wang,J. Li,Y. Hsu, Y. Wu,Y. Lai,M. Chen,Dielectric properties and microstructures of non-reducible high-temperature stable X9R ceramics, Journal of the European Ceramic Society 33 (2013) 1793-1799 .

[6]G. Yao, X. Wang, Y. Zhang, Z. Shen, L. Li, Nb-modified $0.9BaTiO_3$-$0.1(Bi_{0.5}Na_{0.5})TiO_3$ ceramics for X9R high-temperature dielectrics application prepared by coating method, Journal of the American Ceramic Society 95 (2012) 3525-3531.

[7]B. Tang, S. Zhang, X. Zhou, Y. Yuan, L. Yang, Preparation and modification of high Curie point $BaTiO_3$-based X9R ceramics, Journal of Electroceramics 25 (2010) 93-97.

[8]S. Gao, S. Wu , Y . Zhang , H . Yang, X. Wang , Study on the microstructure and dielectric properties of X9R ceramics based on $BaTiO_3$, Materials Science and Engineeing B: Advanced Functional Solid-State Materials 176 (2011) 68-71 .

[9]L. Li, Y. Han, P. Zhang, C. Ming, X. Wei, Synthesis and characterization of $BaTiO_3$-based X9R ceramics, Journal of Materials Science 44 (2009) 5563-5568

[10]E.A. Patterson, D.P. Cann, Relaxor to ferroelectric transitions in $(Bi_{1/2}Na_{1/2})TiO_3$-$Bi(Zn_{1/2}Ti_{1/2})O_3$ solid solutions, Journal of the American Ceramic Society 95(2012) 3509-3513.

[11]]N. Raengthon, H.J. Brown-shaklee, G.L. Brennecka, Dielectric properties of $BaTiO_3$-$Bi(Zn1/2Ti_{1/2})O_3$ -$NaNbO_3$ solid solutions,Journal of Materials Science 48(2013)2245-2250

[12]S.C. Jeon, C.S. Lee, S.J.L. Kang, The mechanism of core/shell structure formation during sintering of BaTiO3-based ceramics, Journal of the American Ceramic Society 95(2012)2435-2438.

[13]A.Zeb and S. J. Milne,Stability of High Temperature Dielectric Properties for $(1-x)Ba_{0.8}Ca_{0.2}TiO3$-$xBi(Mg_{0.5}Ti_{0.5})O_3$ Ceramics, Journal of the American Ceramic Society 96(2013)2887-2892

[14]A.Zeb and S. J. Milne, Low variation in relative permittivity over the temperature range 25-450□ for ceramics in the systerm $(1-x)[Ba_{0.8}Ca_{0.2}TiO_3]$-$x[Bi(Zn_{0.5}Ti_{0.5})O_3]$,Journal of the European Ceramic Society 34(2014)1727-1732

[14]L. Zhang, O.P. Thakur, A. Feteira, G.M. Keith, A.G. Mould, D.C. Sinclair, A.R. West, Comment on the use of calcium as a dopant in X8R $BaTiO_3$-based ceramics, Applied Physics Letters 90 (2007)142914.

[15]S. Wang, S. Zhang, X. Zhou, B. Li, Z. Chen, Influence of sintering atmosphere on the microstructure and electrical properties of $BaTiO_3$-based X8R materials, Journal of Materials Science 41 (2006) 1813-1817.

[16]L. Li, R. Fu, Q. Liao, L. Ji, Doping behaviors of NiO and $Nb_2O_5$ in $BaTiO_3$ and dielectric properties of $BaTiO_3$-based X7R ceramics, Ceramics International 38 (2012) 1915-1920.

[17]Yasukawa K,Nishimura M, Nishihata Y,et al,Core-shell structure analysis of $BaTiO_3$ ceramics by synchrotron X-ray diffraction,J. Am. Ceram. Soc., 90(2007)1107-1111 .

[18]C.J.Stringer,T.R.Shrout, and C.A.Randall, High-temperature perovskite relaxor ferroelectrics: A comparative study, J.Appl.Phys, 101(2007)054107

[19]V. A. Isupov, Causes of Phase-Transition Broadening and the Nature of Dielectric Polarization Relaxation in Some Ferroelectrics, Sov. Phys. Solid State, 5 (1963)136-140 .

[20]G. A. Smolenski, Physical Phenomena in Ferroelectrics With Diffused Phase Transition, J. Phys. Soc. Jpn. , 28(1970)26-37.

[21]D. Völtzke, H. Abicht, Mechanistic investigations on the densification behaviour of barium titanate ceramics, Solid State Sciences 3 (2001)417-422.

[22]V. A. Isupov, Causes of Phase-Transition Broadening and the Nature of Dielectric Polarization Relaxation in Some Ferroelectrics, Sov. Phys. Solid State, 5 (1963)136-140.

[23]G. A. Smolenski, Physical Phenomena in Ferroelectrics With Diffuse d Phase Transition, J. Phys. Soc. Jpn. , 28(1970)26-37.

[24]Aniya M, J.Therm. Anal.Calorim,69(2002) 971.

[25]Vilgis T A ,J.Phys.Cond.Matter ,2(1990) 3667.

[26]W.Q.Cao, M.F.Shu, Bond energy and coordination number model for relaxor ferroelectrics, Acta Phys.Sin., 62(2013)017701.

[27]Y. Sun,H. Liu,H. Hao,L. Zhang,The role of Co in the $BaTiO_3$-$Na_{0.5}Bi_{0.5}TiO_3$ based X9R ceramics, Ceramics International,41(2015) 931-939.

[28]T. Wang, L. Li, C. Li, Q.Y. Hu,and X.Y. Wei, Relaxor Ferroelectric $BaTiO_3$-$Bi(Mg_{2/3}Nb_{1/3})O_3$ Ceramics for Energy Storage Application, J. Am. Ceram. Soc.,(2014)1-8.

[29]S.C. Jeon,B.K. Yoon,K.H. Kim,S.J.L. Kang, Effects of core/shell volumetric ratio on the dielectric-temperature behavior of $BaTiO_3$, Journal of Advanced Ceramics,2014,3(1)76-82

[30]R. D. Shannon, Revised Effective Ionic Radii and Systematic Studies of Interato mic Dist ances in

Halides and Chalc ogenides, Acta Crystallogr. A, 32(1976)751-67 .

[31]D.Hennings,Barium titanate based ceramic materials for dielectric use,Int. J. High technol. Ceram. 3(1987)91-111

[32]N. Zhang, L. Li, J. Chen, J. Yu, ZnO doped $BaTiO_3$-$Na_{0.5}Bi_{0.5}TiO_3$-$Nb_2O_5$-based ceramics with temperature-stable high permittivity from -55℃ to 375℃，Materials Letters 138(2015)228-230

[33]T. Zhang, X. Tang, Q. Liu, Y. Jiang, and X. Huang, Oxygen-Vacancy-Related High Temperature Dielectric Relaxation in $(Pb_{1-x}Ba_x)ZrO_3$ Ceramics, J. Am. Ceram. Soc., (2014)1-8

[34]Hualei Cheng, Hongliang Du, Wancheng Zhou, Dongmei Zhu, Fa Luo, Boxi Xu, $Bi(Zn_{2/3}Nb_{1/3})O_3$-$(K_{0.5}Na_{0.5})NbO_3$ High-Temperature Lead-Free Ferroelectric Ceramics with Low Capacitance Variation in a Broad Temperature Usage Range, J.Am.Ceram.Soc., 96(2013)833-837

[35]A.A.Bokov, Z.-G.YE, Recent progress in relaxor ferroelectrics with perovskite structure, Journal of materials science, 41(2006)31-52

[36]Xiuli Chen, Jie Chen, Dandan Ma, Liang Fang, Huanfu Zhou, Thermally Stable $BaTiO_3$-$Bi(Mg_{2/3}Nb_{1/3})O_3$ Solid Solution with High Relative Permittivity in a Broad Temperature Usage Range, J.Am.Ceram.Soc., 98(2015)804-810

[37]Smolensky G A, Physical phenonmena in ferroelectrics with diffuse phase transition, J.Phys.Soc.Japan, 28(1970):26-37

[38]H. Arvind, K. Umesh, R. E. Newnham, and L. E. Cross, “Stabilization of the Perovskite Phase and Dielectric Properties of Ceramics in the Pb(Zn1/3Nb2/3)O3-BaTiO3 System ,” J. Am. Ceram. Soc. Bull., 66(1987) 671-676.

[39]Z. Li, Q. Li, L. Zhang, and X. Yao, “Die lectric Properties and Transition Temperature of Ceramics in the Pb(Mg1/3Nb2/3)O3-BaTiO3System ,” Ferroelectrics , 262(2001)47-52.

[40]C. C. Huang and D. P. Cann, “Phase Tra nsition and Dielectric Properties in Bi(Zn1/2Ti1/2)O3-BaTi O3,” J. Appl. Phys., 104 , 024117, 4pp (2008).

[41] M. R. Suchomel and P. K. Davies, “Enhanced Tetragona lity in (x)PbTiO3-(1-x)Bi(Zn1/2Ti1/2)O3 and Related Solid Solution System s,” Appl.Phys. Lett. , 86, 262905, 3pp (2005).

[42] B. Xiong, H. Hao, S. J. Zhang, H. X. Liu, and M. H. Cao, “Structure,Dielectric Properties and Temperature Stability of BaTiO3-Bi(Mg1/2Ti1/2)O3 Perovskite Solid Solutions, ”J. Am. Ceram . Soc., 94 (2011)3412-3417.

[43] J. Chen, X. L. Tan, W. Jo, and J. R €odel, “Temperature Dependence of Piezoelectric Properties of

High -Tc (1-x)Bi(Mg1/2Ti 1/2)O3–XPbTiO3," J. Appl.Phys., 106(2009) 034109, 7pp .

[44] T. Le ist, J. Chen, W. Jo, E. Aulbach, J. Suffner, and J. R €ode, "Temperature Dependence of the Piezoelectric Coefficient in BiMeO3-PbTiO3 (Me = Fe,Sc, (Mg1/2Ti1/2)) Ceramics," J. Am. Ceram.Soc., 95 (2012)711-715.

[45] C. SM, S. CJ, S . TR, and R. CA, "Structure and Property Investigation of A Bi-Based Perovskite Solid Solution: (1-x)Bi(N i1/2Ti1/2)O3– XPbTiO3,"J. Appl. Phys., 98(2005)034108, 4pp .

[46] Y. L. Wang, X. L. Chen, H. F. Zhou, L. Fang, L. J. Liu, and H. Zhang,"Evolution of Phase Transformation Behavior and Dielectric Temperature Stability of BaTiO3-Bi(Zn0.5Zr0.5)O3 Ceramics System," J. Alloy. Compd. , 551 (2013)365-369.

[47]A. Zeb and S. J. Milne, "Temperature-Stable Dielectric Properties From -20 to 430$^{o}$C in the System BaTiO3–Bi(Mg0.5Zr0.5)O3," J. Eur. Ceram . Soc. ,34(2014)3159-3166.

# Figures

Figure 1.The locations of the compositions in the $Bi^{3+}$,$Na^{+}$,$Zn^{2+}$,$Nb^{5+}$ doped $BaTiO_3$ dielectric system

Figure 2.(a)-(b) Temperature dependence of dielectric constant and capacitance variation rate based on $C_{25^oC}$ for samples with various amounts of $Bi(Zn_{2/3}Nb_{1/3})O_3$, sintered at 1200°C, measured at 1kHz; (c) The sample doped with x=0.27 of $(1-x)BaTiO_3$-$xBi(Zn_{2/3}Nb_{1/3})O_3$-$0.015NaNbO_3$ system, sintered at 1200°C, measured at 1kHz-1MHz; (d) Plot of $\ln(1/\varepsilon-1/\varepsilon_m)$as a function of ln(T-Tm) for $(1-x)BaTiO_3$ -$xBi(Zn_{2/3}Nb_{1/3})O_3$ -$0.015NaNbO_3$ (x=0.22,0.24, 0.27, 0.30, sintered at 1200°C)at 1kHz.

Figure 3.The micro-mechanism in the $Bi^{3+}$,$Na^{+}$,$Zn^{2+}$,$Nb^{5+}$ doped $BaTiO_3$ dielectric system, benefiting to the realization of ultra-wide temperature stability.

Figure 4.(a) X-ray diffraction patterns of $(1-x)BaTiO_3$-$xBi(Zn_{2/3}Nb_{1/3})O_3$-$0.015NaNbO_3$ ceramics with x=0.22,0.24,0.27,0.30 at room temperature; (b) the (002)/(200) diffraction patterns of the sample in the range 44°-46°; (c) compositional dependence of the tetragonality factor (c/a).

Figure 5.The relationships between sintering temperatures and densities of all studied samples.

Figure 6. SEM micrographs of natural surfaces for $(1-x)BaTiO_3$-$xBi(Zn_{2/3}Nb_{1/3})O_3$-$0.015NaNbO_3$ ceramics with x=0.22,0.24,0.27,0.30 : (a)-(d).

Figure 7. (a)-(d)The dictribution of the grain size in $(1-x)BaTiO_3$-$xBi(Zn_{2/3}Nb_{1/3})O_3$-$0.015NaNbO_3$ ceramics with x=0.22,0.24,0.27,0.30; (e)compositional dependence of the grain size.

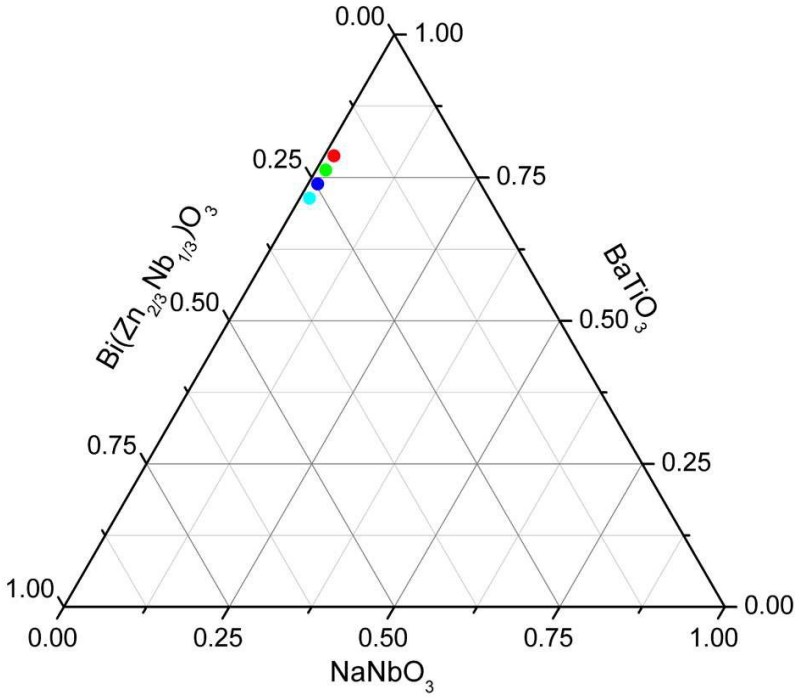


Fig.1

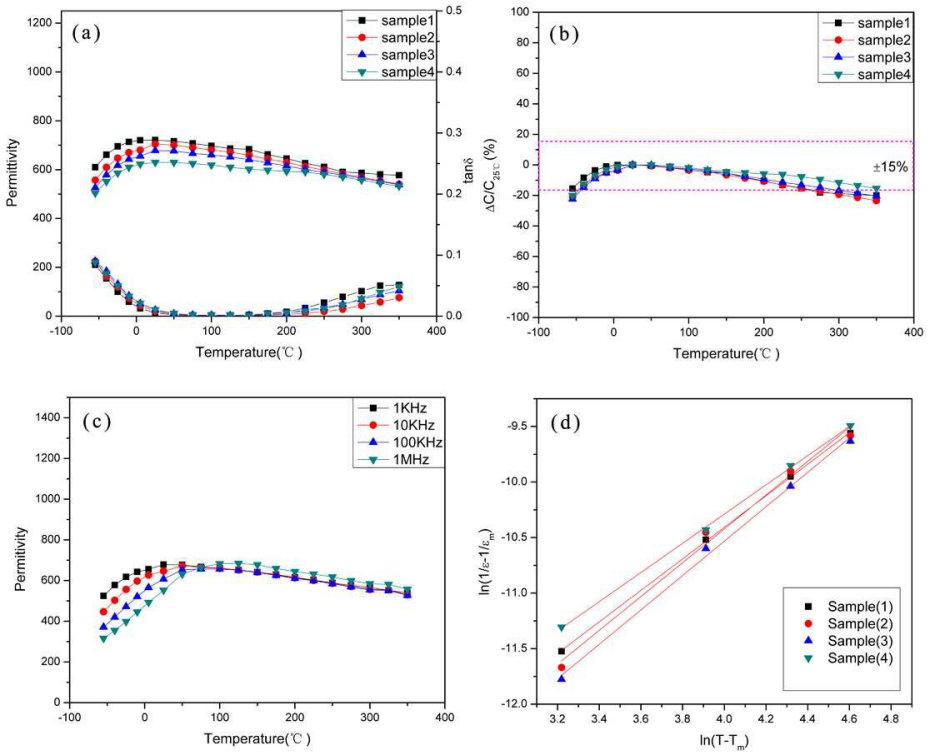


Fig.2

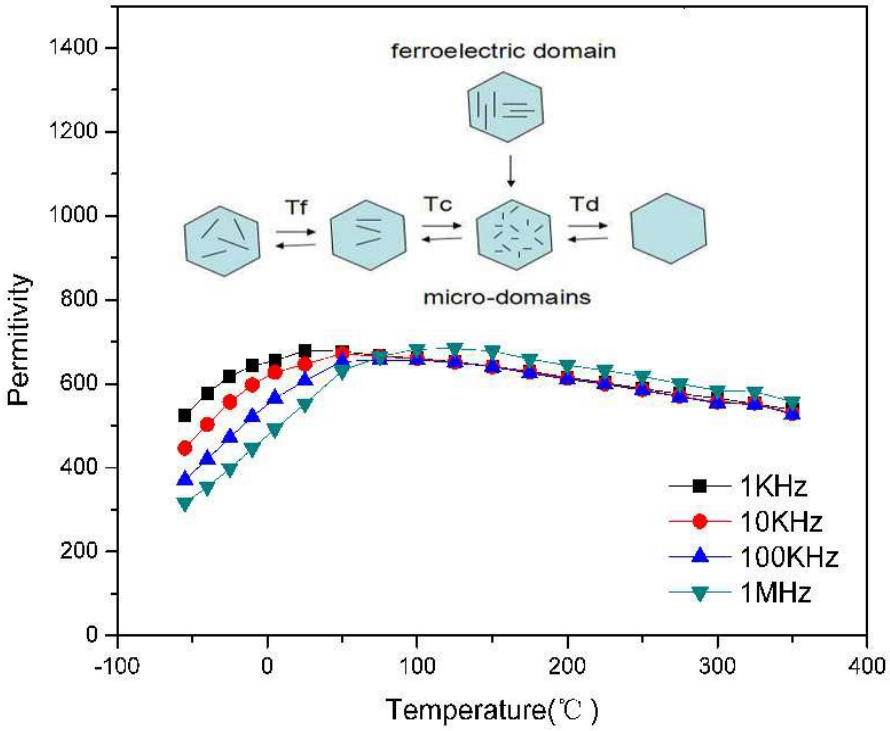


Fig3

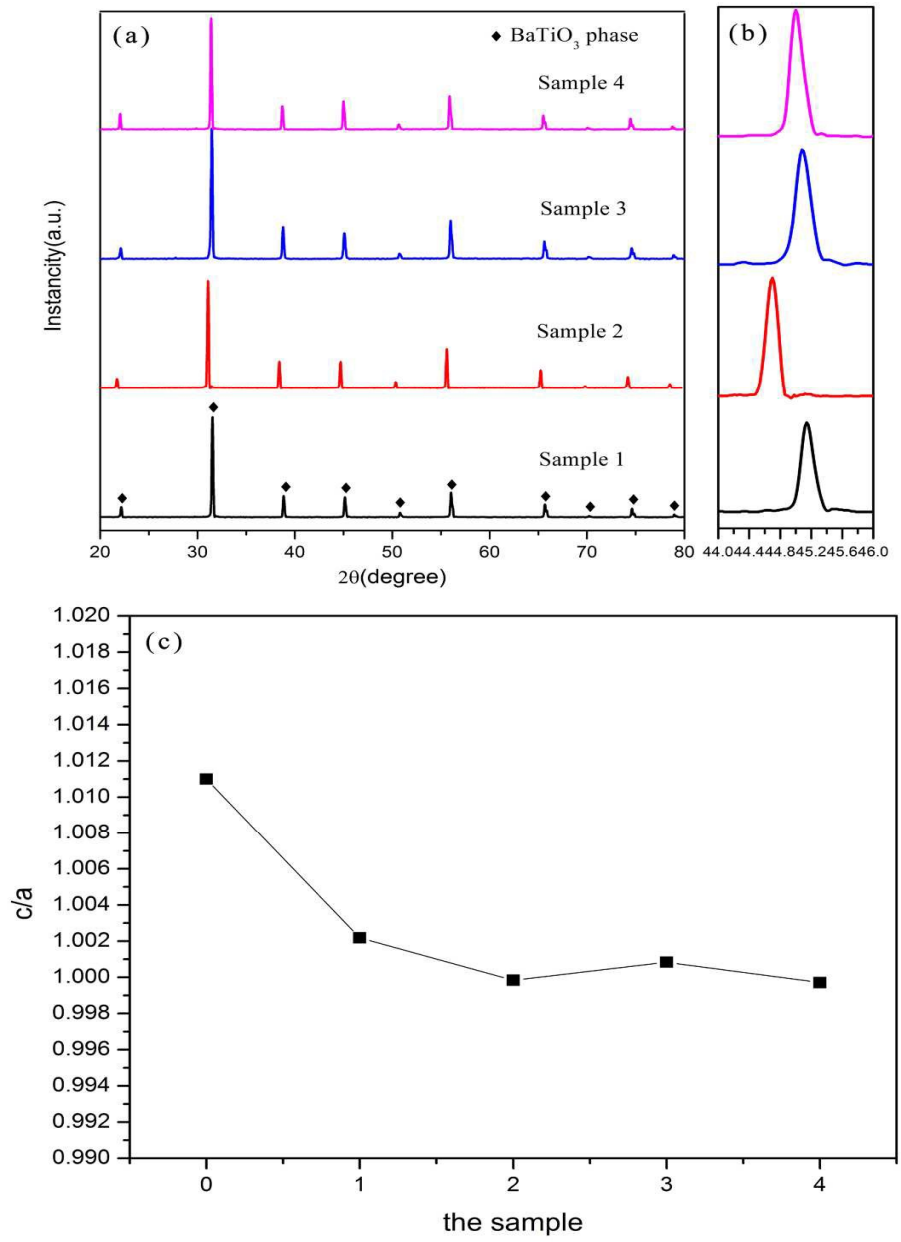


Fig.4

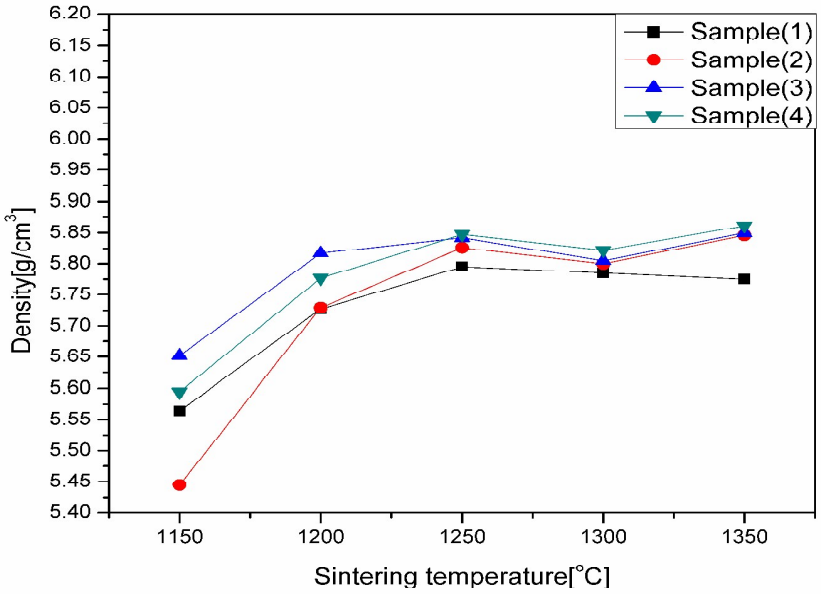


Fig.5

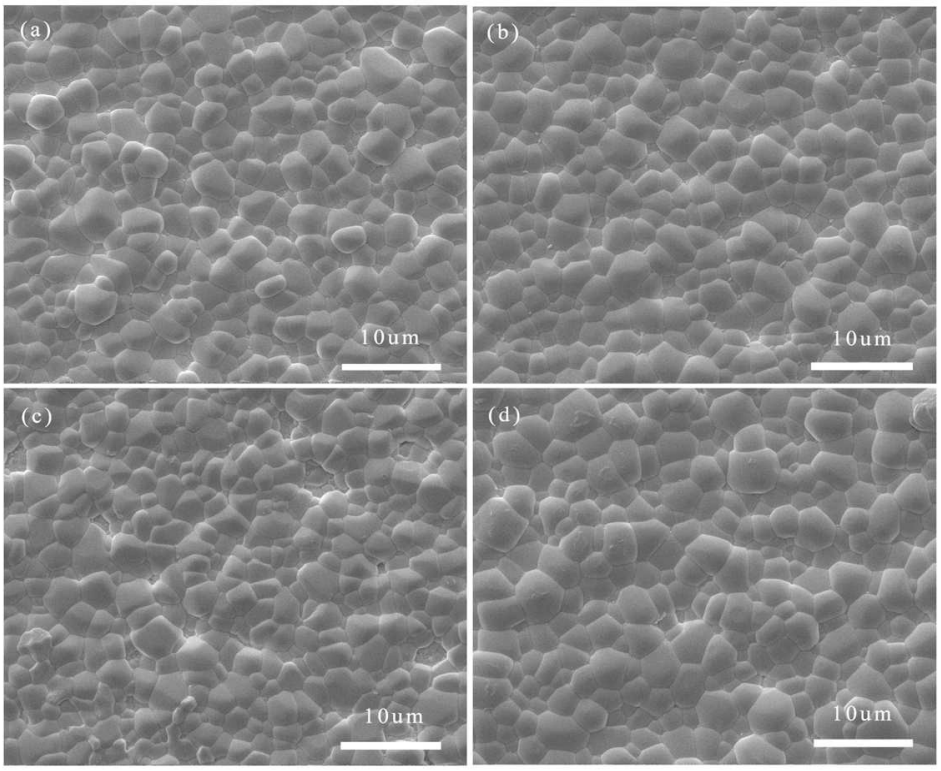


Fig.6

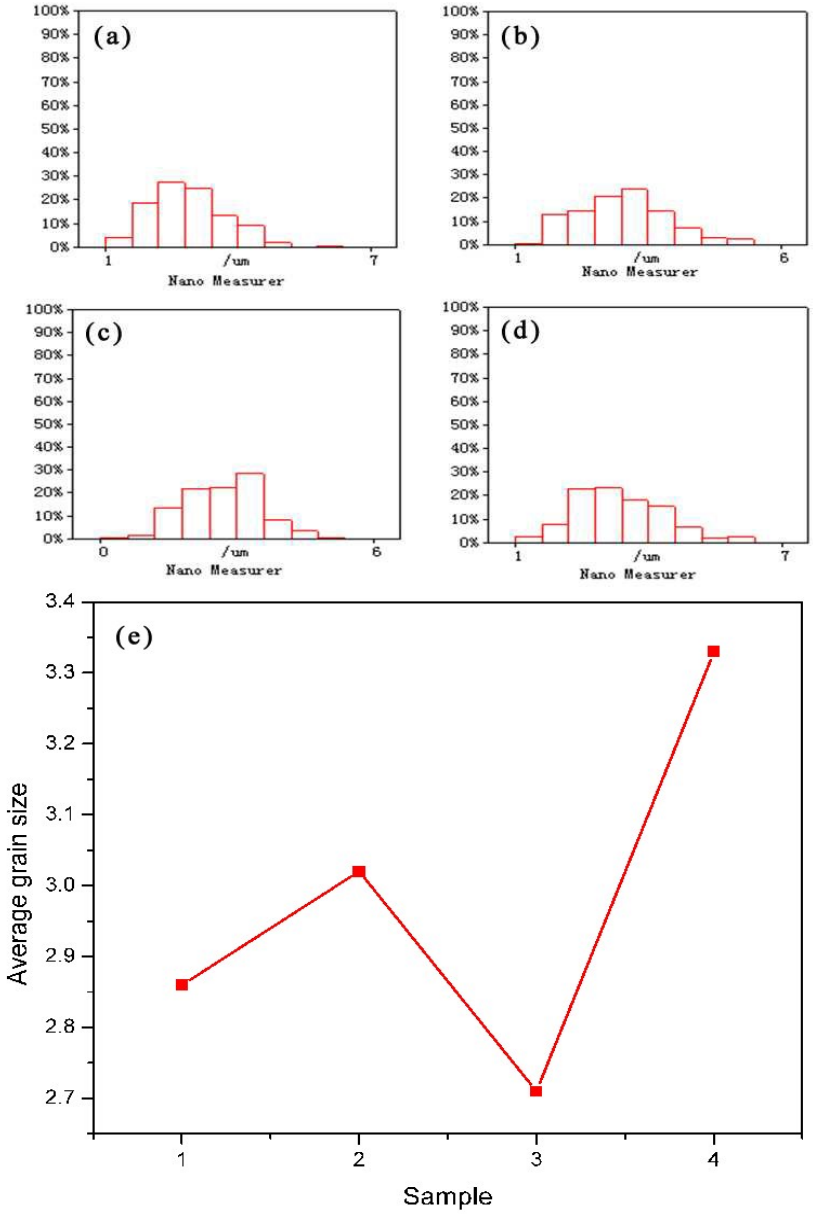


Fig 7

Table 1 Comparisons of Varying amounts of $Bi(Zn_{2/3}Nb_{1/3})O_3$ (x=0.25,0.275,0.3, 0.325) sintered at 1200°C

| Sample | $\varepsilon_r$ at 25°C | tan δ | $\Delta C/C_{25℃}$(%)≤±15% | | Curie temperature (Tc / °C) | Bulk density ($g/cm^3$) | Insulation resistance ($\rho_v$ $10^{10}$ Ω cm) |
|---|---|---|---|---|---|---|---|
| 1 | 721 | 0.00539 | -55°C | 245°C | 25 | 5.729 | 2.78 |
| 2 | 704 | 0.00773 | -50°C | 250°C | 25 | 5.727 | 3.74 |
| 3 | 678 | 0.01005 | -50°C | 300°C | 25 | 5.817 | 1.41 |
| 4 | 630 | 0.01069 | -53°C | 350°C | 50 | 5.777 | 4.25 |

In this paper, the micro-mechanism in the (1-x)$BaTiO_3$-x$Bi(Zn_{2/3}Nb_{1/3})O_3$-0.01$NaNbO_3$ system, benefiting to the realization of ultra-wide temperature stability, was proposed and applied to study the dielectric properties. What's more, the bond energy and coordination number model was used to investigate the .the relaxation behavior, which is rarely investigated until now.